European Research Infrastructure supporting Smart Grid and Smart Energy Systems Research, Technology Development, Validation and Roll Out – Second Edition

Project Acronym: **ERIGrid 2.0**

Project Number: **870620**

Technical Report Lab Access User Project

Control and Power Hardware-in-the-Loop Testing of Grid-Forming Voltage Source Converters (CPHILT-GFVSC)

Access Duration: 20/09/2022 to 28/10/2022

Funding Instrument:	Research and Innovation Action
Call:	H2020-INFRAIA-2019-1
Call Topic:	INFRAIA-01-2018-2019 Integrating Activities for Advanced Communities
Project Start:	1 April 2020
Project Duration:	54 months
User Group Leader:	José María Maza-Ortega (Universidad de Sevilla)

This project has received funding from the European Union's Horizon 2020 research and innovation programme under Grant Agreement No. 870620.

Report Information

Document Administrative Information	
Project Acronym:	ERIGrid 2.0
Project Number:	870620
Access Project Number:	05.145-2022
Access Project Acronym:	CPHILT-GFVSC
Access Project Name:	Control and Power Hardware-in-the-Loop Testing of Grid-Forming Voltage Source Converters
User Group Leader:	José María Maza-Ortega (Universidad de Sevilla)
Document Identifier:	ERIGrid2-Report-Lab-Access-User-Project-CPHILTGFVSC-final
Report Version:	v1.1
Contractual Date:	28/11/2022
Report Submission Date:	19/03/2023
Lead Author(s):	Manuel Barragán-Villarejo (Universidad de Sevilla)
Co-author(s):	Francisco Jesús Matas-Díaz (Universidad de Sevilla), Alkistis Kontou (ICCS-NTUA)
Keywords:	Grid-forming capability, Inertial Response, Virtual Synchronous Generators, Single-Phase, Voltage Source Converter, European Union (EU), H2020, Project, ERIGrid 2.0, GA 870620
Status:	__ draft, _x_ final

Change Log

Date	Version	Author/Editor	Summary of Changes Made
21/03/2023	v1.0	Manuel Barragán-Villarejo (Universidad de Sevilla), Francisco Jesús Matas-Díaz (Universidad de Sevilla), Alkistis Kontou (ICCS-NTUA)	Draft report
22/03/2023	v1.1	Alkistis Kontou (ICCS-NTUA)	1st Review

Table of Contents

List of Figures

List of Tables

List of Abbreviations

LA Lab Access
UP User Project

Executive Summary

The integration of renewable energy resources (RES) in power systems is displacing conventional generation assets based on synchronous generators. RES use voltage source converters (VSCs) as the main interface between the primary energy source and the grid. Therefore, these power electronic devices should guarantee in future converter-dominated power systems, robust and secure operation. For this purpose, the provision of ancillary services is of particular relevance, especially concerning frequency regulation. Recently, the concept of a virtual synchronous generator (VSG) with grid-forming functionality has emerged to operate in three-phase systems. However, the extension of this concept to single-phase devices, especially those operating within low-voltage networks, has not been widely explored. Taking into account that a relevant part of the new RES generation is connected to distribution systems, it might be necessary to endow a certain number of single-phase RES with grid-forming capability. This work proposes the use of two reference frames, rotating and stationary, to implement the control levels of a single-phase network forming VSC. These levels are made up of inner and outer control loops that allow the grid-forming VSC to adapt its voltage at the POI according to the load of the system.

The rotating reference frame for single-phase systems is generated through virtual axes dq. These are obtained by means of a filter to the voltages and currents of the system. This makes it possible to implement classic control strategies based on PI controls. While the stationary reference frame is based on the currents and voltages of the single-phase system, implementing PR controllers in the inner control loops to track sinusoidal references.

The evaluation and transfer of code between the User Group and the Host Group has been carried out using the following methodology:

- Simulations carried out by the User Group with the aim of validating the control of single-phase GF VSC in the proposed reference frameworks.
- Transfer and adaptation of the User Group simulations to the Host Group simulation environment. The host group has a detailed simulation of the Triphase converter, device used in the experimental test-bed, which has been provided by Triphase. This simulation allows to integrate all the control blocks identically to the files used for the experimental validation.
- Comparison of the dynamic and steady state response of the single phase GF VSC in both reference frames between the User Group simulations and the simulation environment used by the Host Group. To carry out this comparison process, an analysis of the performance of each level is carried out individually. This allows evaluating each level of control separately as well as its behavior.
- Experimental evaluation of the single-phase GF VSC for both frames of reference. The control is progressively validated by increasing voltage levels and currents in the prototype. In this way, control performance for both reference frames is safely and progressively evaluated. Similar to the previous stage, each level of control is validated individually.

In addition, it was discussed how to implement the evaluation of the single-phase GF VSC in isolation mode for a P-HIL environment. This discussion revolved mainly around how to emulate a passive load through an amplifier. Several strategies were established, which are being evaluated in a simulated environment.

The simulation results of the User Group show an adequate dynamic response and good power

quality for each of the control levels in both reference frames. However, the dynamic response of the stationary frame is faster than the rotating axes. This is due to the delay introduced into the control by the filter that generates the rotating virtual reference frame in *dq* axes. Identical responses are obtained with the simulation results of the Host Group once the code transfer was performed. The dynamic and steady-state response of each control level in the experimental results of the single-phase GF VSC presents a very similar behavior to those obtained in both simulations. The only appreciable difference is relative to the minimum value of the frequency reached with an increase in load. This value is reached in simulation for the rotating frame, while in the experimental results it is reached for the stationary frame. Both groups believe that the mismatch is due to a difference in the gains of some control stage. However, further research on this question remains pending.

It can be concluded that a work methodology has been established for the transfer of research from the User Group to the experimental validation in the laboratory infrastructure of the Host Group. This methodology has allowed to successfully validate the single-phase GF VSC control in two reference frames. In addition, there have been discussions between both groups about the best way to implement a load in P-HIL for isolated systems. These discussions have also led to how to validate through P-HIL the control of a GF VSC in a grid-connected mode. As a consequence, both groups have agreed to participate in a new ERIGrid call for the year 2023 with the aim of proposing solutions to these open questions during the execution of this project.

1 Lab-Access User Project Information

1.1 Overview

Table 1 collects relevant information of the project, host infrastructure and user member groups during the period where the project was developed.

Table 1: Table with relevant information of the Project

User Project Acronym	CPHILT-GFVSC
User Project Title	Control and Power Hardware-in-the-Loop Testing of Grid-Forming Voltage Source Converters
Main Scientific/Technical Field	Control of converter interface renewable energy sources
Host Infrastructure	Electric Energy Systems Laboratory (ICCS-NTUA)
Acces Period	20.9.22-28.10.22
User Group Members	José María Maza-Ortega, Manuel Barragán-Villarejo Francisco Jesús Matas-Díaz from Universidad de Sevilla

1.2 Research Motivation, Objectives, and Scope

The main motivation of the project is to provide technical solution in converter-interfaced renewable energy sources (CI-RES) that provide ancillary services to the network in order to operate the future power systems with the same security and robustness guarantees as the current one. For this, it is proposed to operate the CI-RES in grid-forming (GF) mode capable of emulating virtual synchronous generators both in isolated systems and grid-connected mode. To evaluate the performance of the grid-forming CI-RES, it is proposed to sequentially validate the GF mode in CI-RES via simulation, C-HIL and P-HIL for different types of networks. Therefore, the specific objectives of the project defined in the proposal are:

- C-HIL validation of each control level of a GF voltage source converter (VSC) in islanded and grid-connected system with different SCRs and X/R ratios. In this way, it can be guaranteed that the proposed control strategy is robust, which is key before undertaking validations with power devices.
- P-HIL validation of each control level of a GF VSC in an islanded system. A test protocol will be established to ensure the correct experimental validation of the proposed controller for each control layer.
- Analysis of the deviations of C-HIL and P-HIL with respect to the simulation results.
- Robust and stable control design of GF VSC which will facilitate the penetration of renewable energy sources within the power system.
- Standardized testing procedure to validate the control level of a GF VSC in a C-HIL and P-HIL environment.
- At least one paper in a high-impact journal indexed in JCR.

According to the motivation and objectives of the project, the overall scope of the project is to validate the operation of a grid-forming VSC in isolated mode and establish a validation protocol in C-HIL and P-HIL.

The specific objectives were modified during the development of the project. These were re-adapted according to the required test cases and use cases for the specific experimental validation, as well as for safety reasons. More specifically:

- Development of two control approaches for single-phase GF VSCs. One of them based on rotating axes *dq* and another based on stationary axes.
- The purpose of a CHIL experiment is to validate the controller of an actual hardware inverter in safe environment and in conditions close to real. In the case of ICCS, C-HIL is realised through the RTDS real-time control platform and a DSP. However, the experimental validation of the GF VSC was carried out using a controller provided by Thriphase whose microcontroller and programming is totally different from the C-HIL platform. This led to the conclusion that performing C-HIL as a step prior to experimental validation was not a useful since any control and protection algorithm validate into the DSP would have to be modified and adapted to the Thriphase-microprocessor. As an alternative, the control and protection measures of the GF VSC were implemented in simulations provided by Thriphase, the company that provides the microcontroller and power converter. This model faithfully represents all the components of the converter and control which allows to validate the proposed single GF VSC in this simulated environment.
- Experimental validation. The first part of the validation of the GF VSC is its evaluation in isolated systems. From an experimental point of view, initially the converter has to be validated in a full hardware setup, to assess it's behavior and refine the tuning of the controllers. Therefore, all control levels of a GF VSC were evaluated increasing progressively the voltage levels of the power converter connected to a physical resistor instead of a one simulated in P-HIL.
- Simulations to evaluate how to implement an isolated and networked system through the amplifier in P-HIL.

It should be noted that one of the main objectives, which is to establish a GF VSC evaluation protocol to be tested in P-HIL, has been maintained in the execution of the project. For this, we have participated in a new ERIGrid 2.0 call to test the GF VSC in systems connected to the grid through P-HIL for the year 2023.

1.3 Structure of the Document

This document is organised as follows: Section 2 briefly outlines the state-of-the-art/state-of-technology that provides the basis of the realised Lab Access (LA) User Project (UP). Section 3 briefly outlines the performed experiments whereas Section 4 summarises the results and conclusions. Potential open issues and suggestions for improvements are discussed in Section 5.

2 State-of-the-Art/State-of-Technology

GF VSC have been revealed as a viable solution for enhancing system stability and resiliency power networks with high-RES penetration (Rocabert, Luna, Blaabjerg, & Rodríguez, 2012). To achieve this goal, a control structure composed of several control loops is proposed for these converters. In general, this is usually organized as follows (Rosso, Wang, Liserre, Lu, & Engelken, 2021):

- Outer loop - power synchronization loop and voltage amplitude management. The power synchronization loop oversees the system synchronization, computing the frequency and the angle of a VSG. This can be done through different approaches as droop control (Rocabert et al., 2012), power synchronization control (Zhang, Harnefors, & Nee, 2010), enhanced direct power control (Ndreko, Rüberg, & Winter, 2020), synchronverter (Zhong & Weiss, 2011) or Synchronous power control (Rodríguez, Citro, Candela, Rocabert, & Luna, 2018). These strategies to a greater or lesser extent intend to emulate the SG behavior but with subtle differences in the emulated dynamics and implementation issues. With respect to the voltage amplitude management, which is in charge to compute the VSG virtual electromotive force, three strategies are usually applied: droop control (Rocabert et al., 2012), PI-based control (Rodríguez et al., 2018), and cascaded controls involving droop and PI regulators (Rodriguez, Candela, Citro, Rocabert, & Luna, 2013).
- Inner loop - Calculation of the VSC modulation signal. The inner control loop computes the modulation signals of the VSC. These can be classified into open loop (Ooi & Wang, 1990), single-control loop (Liao & Wang, 2019), multi-loop control loop (Loh & Holmes, 2005) and multi-loop control loop with virtual impedance strategies (Rodriguez et al., 2013). The open loop strategy directly assigns to the modulation signal the angle, frequency and voltage amplitude computed in the outer control loop. This neglects the voltage drop in the VSC coupling filter considering that the voltage at the VSC terminals is identical to the voltage of the point of interconnection (POI). To solve this issue, a single-control loop is proposed to control the voltage at the POI but missing the information of the GF VSC injected current. Multiloop-control strategies, composed of a cascade control for managing both voltages and currents of the VSC, solves the problem being possible to saturate the output current if required. An improved version of the cascade controller is to add a virtual impedance to the multiloop-control strategy, which allows to adapt the output impedance of VSC for enhanced stability and control.

GF VSCs have proven their good performance in networks with a low short-circuit ratio (SCR) (Rocabert et al., 2012). However, in stiff grids with high SCRs, GF VSCs tend to lose synchronism with the grid, since a slight change of the phase difference between the converter and grid voltages can lead to large active power variations (Liao, Wang, Liu, Xin, & Liu, 2019). In addition, the R/X ratio of the power line is usually unknown which brings a significant challenge in designing stable and proper control strategy for GF VSCs (Hu, Shan, Cheng, & Islam, 2022). In order to overcome these shortcomings, this proposal explores the design and P-HIL experimental validation of the outer and inner control loops for GF VSCs whose parameters are computed considering the SCR and R/X ratio of the network. With this regard, to the best knowledge of the members of this user group, some gaps can be found in the state of the art. As a matter of fact, the influence of the electrical network parameters on the stability of the outer and inner control loops and the performance of the controller, i.e. adequate decoupling between active and reactive power and transient response of controlled magnitudes, have not been addressed in a comprehensive manner.

The controller implemented for the GF VSC in the project consist of the outer control loop

proposed in (Kryonidis, Malamaki, Mauricio, & Demoulias, 2022) and the inner control loop proposed in (Matas-Díaz, Barragán-Villarejo, Olives-Camps, Mauricio, & Maza-Ortega, 2022) for isolating systems. Both control loops were designed for 3-phases 3-wires balanced systems and the objective of the user member groups was to validate them in the host infrastructure. However, the power converter available in the NTUA-ICSS laboratories was a single-phase converter. This required adapting previous outer and inner control loops to single-phase systems. For them, two strategies have been adopted to implement the GF VSC in isolated single-phase systems: i) rotating reference frame and, ii) stationary reference frame. Figures 1 and 2 represent the complete controller of the GF VSC in rotating and stationary frames respectively. They show the outer and inner control loops and the equations required to implement each control level. This adaptation of the control implied some deviations with respect to the original Labs Access Proposal. The user member groups were unaware that the power converter available at the NTUA-ICSS facilities was single-phase prior to their visit. Therefore, the first week was dedicated to adapt the controller to single-phase systems and validating it through electromagnetic simulation. Despite this drawback, this adaptation has allowed opening new lines of research since the implementation of GF VSC in single-phase systems has not been studied in depth. In fact, the proposal developed for GF VSCs in rotating and stationary frames during the project has resulted in a first publication submitted to the international conference SEST'23 which has been accepted for full paper submission.

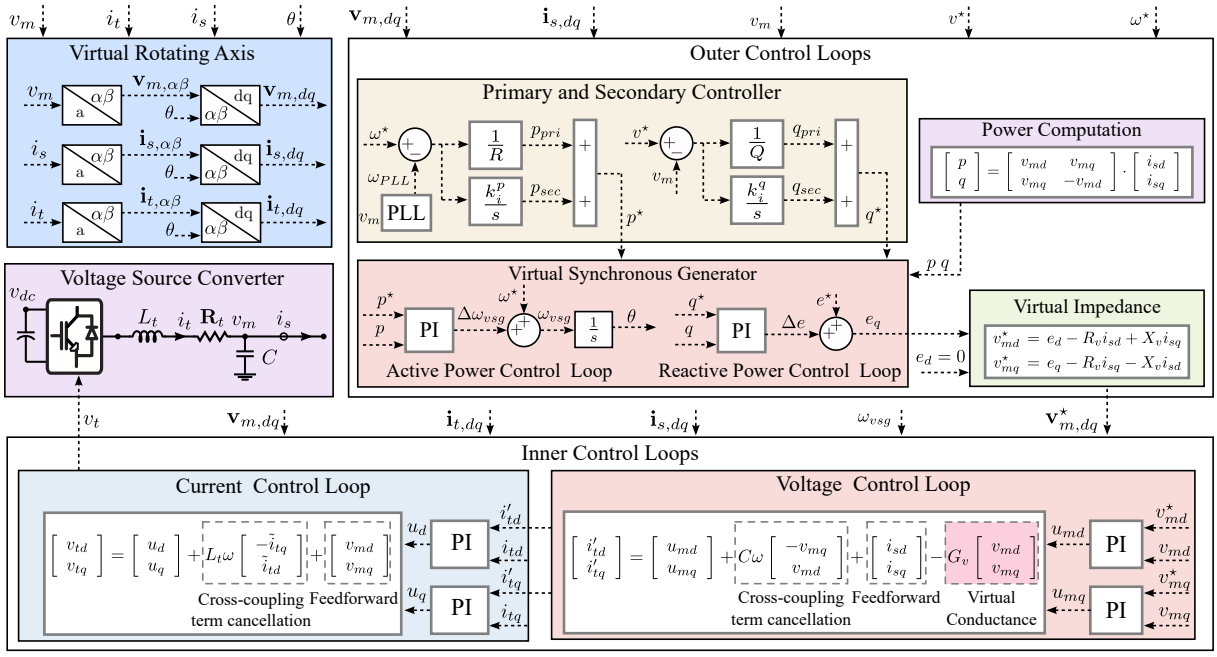

Figure 1: Grid-Forming controller in virtual rotating reference frame (dq axis) for single-phase VSC in isolated systems.

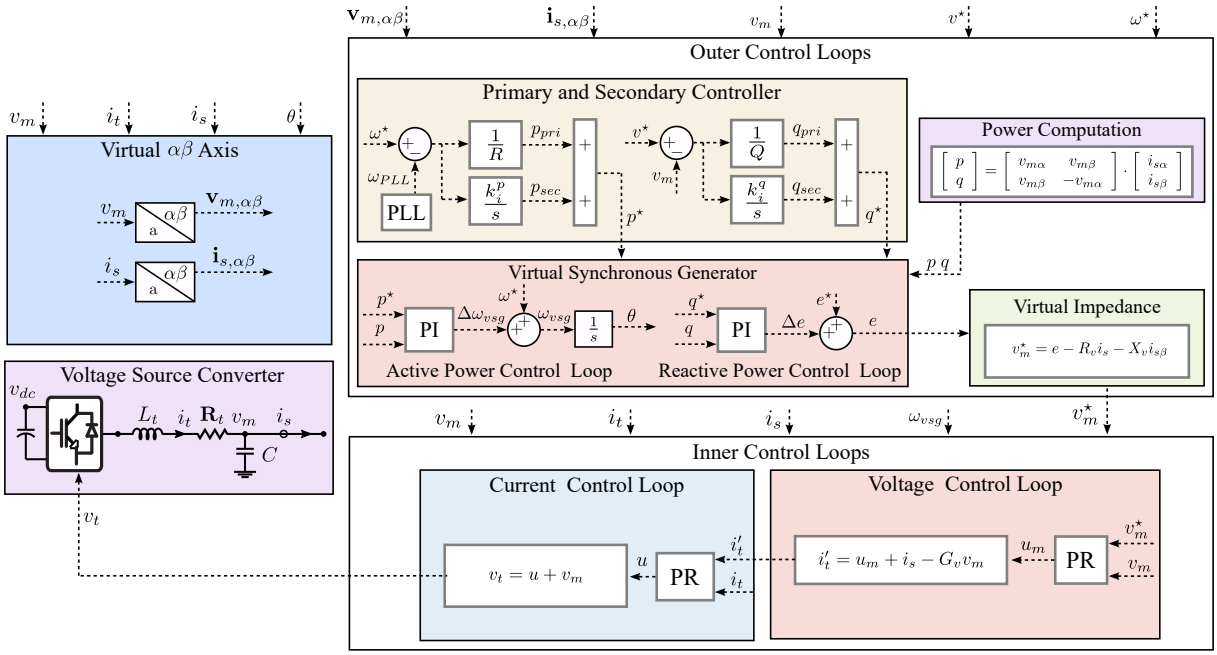

Figure 2: Grid-Forming controller in stationary reference frame for single-phase VSC in isolated systems.

3 Executed Tests and Experiments

3.1 Test Plan, Standards, Procedures, and Methodology

The test plan implemented for validating the GF VSC is described below:

1. Control adaptation from three-phase GF VSC to single-phase GF VSC on rotating and stationary reference axes. Review of the state of the art, control modification of GF VSC and validation through simulation using the source files of the user group. Each control level for single-phase GF VSC in rotating and stationary reference frames was validated by simulation. For this, the dynamic response and steady state response is studied by means of variations of the control references in step cahnge.
2. Transfer of GF VSC control to the simulation file provided by Triphase. Each control level proposed in the previous point is evaluated in the Triphase simulation under the same disturbance. Simulation results are compared between the user group files and the Triphase simulation.
3. Testing of the current control loop in stationary and rotating reference frames of GF converter with Triphase power converter and resistors. Experimental validation of this control level progressively increased the voltage level of the power converter. The power converter voltage is established at low values, the current control loop is evaluated in transient and permanent regime by means of step changes to the current references. The response is compared with the simulation results. If the results are similar in both environments, simulation and experimental, the voltage value of the power converter is progressively increased until reaching the nominal voltage. This procedure is repeated for the rest of the control levels.
4. Testing of the voltage+current control loop in stationary and rotating reference frames with Triphase power converter and resistors. In a similar way to the previous level, the performance of the voltage control is evaluated and compared with the simulation results.
5. Testing of the Primary/Secondary controller and VSG+voltage+current control loop in stationary and rotating reference frames with Triphase power converter and resistors. This is the last control level of GF VSC. This level is evaluated from low voltage to high voltage levels as explained in the testing of the current control loop.
6. Evaluation of how to integrate an isolated system in the RTDS platform and be emulated by the amplifier. This part consisted of studying how to emulate the resistance in P-HIL if through a current source or a controllable voltage source.

3.2 Test Set-up(s)

The set-up of the experimental tests is depicted in Fig. 3 and it is composed of the following components:

- Fully porgrammable power converter provided by Triphase. It was operated as a two level single-phase VSC with a LCL grid-coupling filter. The rated power of the VSC is 15 kVA and its DC bus is maintained by a set of Lead Acid Batteries of 60 V, 250Ah.
- Triphase target PC. This is in charge of receiving analogue measurements from the power converter, voltages and currents, executing the controller of the GF VSC and sending the control signals to the IGBTS drivers of the VSC. This controller is programmed from a

host PC using the software Matlab/simulink. For the real-time monitoring and control of the experiments, a user interface provided by Triphase in Matlab/Simulink was used. This interface allows act on control references, monitoring voltages, currents and inner control variables, as well as save data with high sampling.

- Resistors. These resistors were used as a passive load for the power converter with the objective of evaluating the performance of the proposed single-phase GF VSC.
- Real-time platform provided by RTDS. This platform has not been involved in the development of the experimental results provided in section 4. This began to be used at the end of the project, once the experimental results of section 4 were obtained, to evaluate the option of simulating a passive load in the real time platform RDTS and that it was emulated by a power amplifier in P-HIL. For the emulation of the passive load, different alternatives were evaluated: among them it is worth highlighting the emulation by the amplifier of the circulating current by a passive load simulated in RTDS. Currently, this alternative and others that allow the reproduction of any type of load in a P-HIL environment are being evaluated. The emulation of a passive load and an electrical network through P-HIL to evaluate the performance of the single phase GF VSC are pending works of this project. To conclude the execution of this work, we have participated in a new ERIGrid 2.0 call for the year 2023.

Figure 3: Triphase 15kV configurable power converter operated as single phase inverter connected to a resistive load bank.

3.3 Data Management and Processing

Triphase provides a controller that can communicate through a beckoff card with the RTDS of the laboratory. RTDS was used in that setup only for data recording and real-time monitoring purposes. The data was saved in csv extension which allows it to be processed by Matlab, python or any other mathematical software. The results presented in next section are processed using a python code which processes the results saved in the csv files.

Regarding data management, it has been saved in a shared cloud between the two institutions provided by onedrive.

4 Results and Conclusions

4.1 Discussion of Results

Tests implemented during the Lab Access User Project follow the plan described in section 3. Due to the adaptation of the GF control from three-phase to single-phase systems, the first group of tests consisted in evaluating the performance of each control level in simulation. In order to reduce the description of this part of the work, which does not involve experimental results, the analysed results of the single-phase GF VSC in stationary and rotating frames correspond to the evaluation of all control levels described in Fig. 1 and Fig. 2 when the load connected to the VSC is modified from 1 kW to 2 kW at second 30 of the simulation.

Figure 4 shows the simulation results of the single-phase GF VSC in rotating and stationary frames using the simulation files of the user group. The top plots represents from left to right the current references and current injected by the VSC in the virtual *dq* axes of the rotating frame, the voltage references and voltage imposed by the VSC at the POI in the virtual *dq* frame and the frequency of the system for rotating and stationary frames. While, the bottom plots from left to right illustrates the current references and current injected by the VSC in the stationary frame, the voltage references and voltage imposed by the VSC at the POI in stationary frame and the active power supplies to the load and the active power reference in rotating and stationary frames.

With respect to the tracking of the references in currents and voltages for both frames, an adequate tracking is observed in steady-state before and after the load change. However, there are some differences in the dynamic response when the load is changed at the 30 second. For the rotating frame, voltage and current references presents overshoot and under damping. However, the references in the stationary frame vary smoothly. In addition, the tracking of the references in stationary frame are faster than rotating frame. The dynamic response of the inner loops affects the dynamic performance of the outer loops. A faster recovery of the frequency is observed in the stationary frame than in the rotating frame, despite the fact that the gains of the controllers in the outer loops are identical for both frames. Moreover, the Nadir is lower in stationary frame. This behaviour is also reflected in the active power injected by the VSC. The power injected by the rotating frame has an overshoot compared to the power supplied with stationary frames.

The reason that leads to a dynamic difference between both reference frames corresponds to the generation of the virtual *dq* components. To obtain these components, it is necessary to introduce a filter to the voltages and current magnitudes whose dynamics affect all the control loops of the GF VSC. However, the stationary frame, the natural one of a single-phase system, the controller is directly applied on the sinusoidal currents and voltages without including any filter for these components. Therefore, no additional dynamics are added to the inner and outer control loops that affect the performance of the single-phase GF VSC.

The second group of tests are again simulation results. These correspond to the results obtained with the implementation of single-phase GF VSC in stationary and rotating frames on the simulation files provided by the host laboratory. This file contains an exact model of the Triphase power converter which is used for the experimental tests.

In order to evaluate if the implementation of the single-phase GF VSC controller in the Triphase model was carried out correctly, a comparison of the dynamic response of the inner control loops in the two simulation environments was made: i) simulation with the files of the User Group and, ii) simulation of the Triphase provided by the host group.

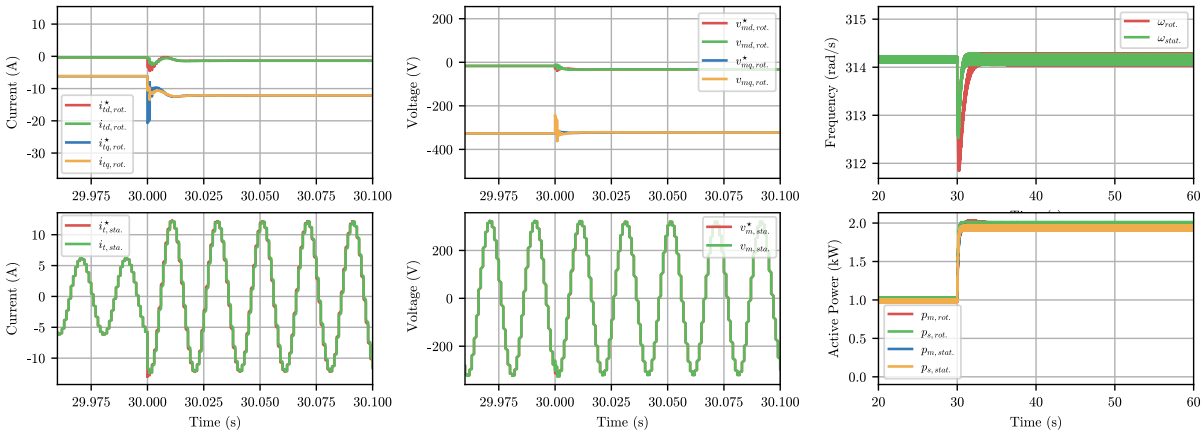

Figure 4: Simulation results of the single phase GF VSC under load power increase. Tracking of the current and voltages in rotating frame and stationary frame. Active power tracking and frequency evolution in both frames.

Figure 5 depicts the results of the voltage control loop when the reference voltage $v^{\star}_{mq}$ in the rotating frame is changed from 0 to 50 V and from 50 to 100 V. The top figure corresponds to the results from the simulation files of i) and the bottom figure shows the results from ii). The results show identical dynamic and steady-state behaviour, which indicates that both simulations are modelling the control and power elements (power converter, filters, etc.) present in the system with the same level of accuracy.

Figure 6 shows a comparison of the voltages in stationary frame between simulations i) and ii). The top plot represents the comparison of the voltages with a step change of the voltage reference $v^{\star}_{m}$ from 0 to 50 V. The bottom plot shows identical magnitudes with a step change from 50 to 100 V. The acronym SIMS correspond to simulation i) and, TRI is assigned with simulation file ii). The results reflect that the voltages are overlapped, therefore, it can be concluded that the transfer of control from the files i) to ii) has been carried out successfully also in the stationary frame.

Once the simulation results showed the expected response of the single-phase GF VSC control in both reference frames, each control loop was evaluated independently on the experimental set-up:

4.1.1 Current control loop

This loop is dedicated to control the current supplied to the resistor from the Triphase converter. Firstly, the results in dynamic regime are shown with the objective of evaluating the tracking of the controller and, then, the results in steady state to evaluate the power quality of the injected currents.

The tracking of the currents under a reference step change of 2 A in the reference current $I^{\star}_{q}$ for the virtual axes dq of the rotating frame are shown in Fig. 7. The current I_q shows a adequate tracking of the reference with a good degree of decoupling, that is, the current I_d is hardly disturbed by the reference step change of $I^{\star}_{q}$. However, the dynamic response is shown to be too slow since it takes about 1 second to reach the steady-state. The reason for this slow dynamic is due to the integral gain of the PI controller on dq axes. This is computed using the value of the internal resistance of the coupling inductor. However, in this isolated system,

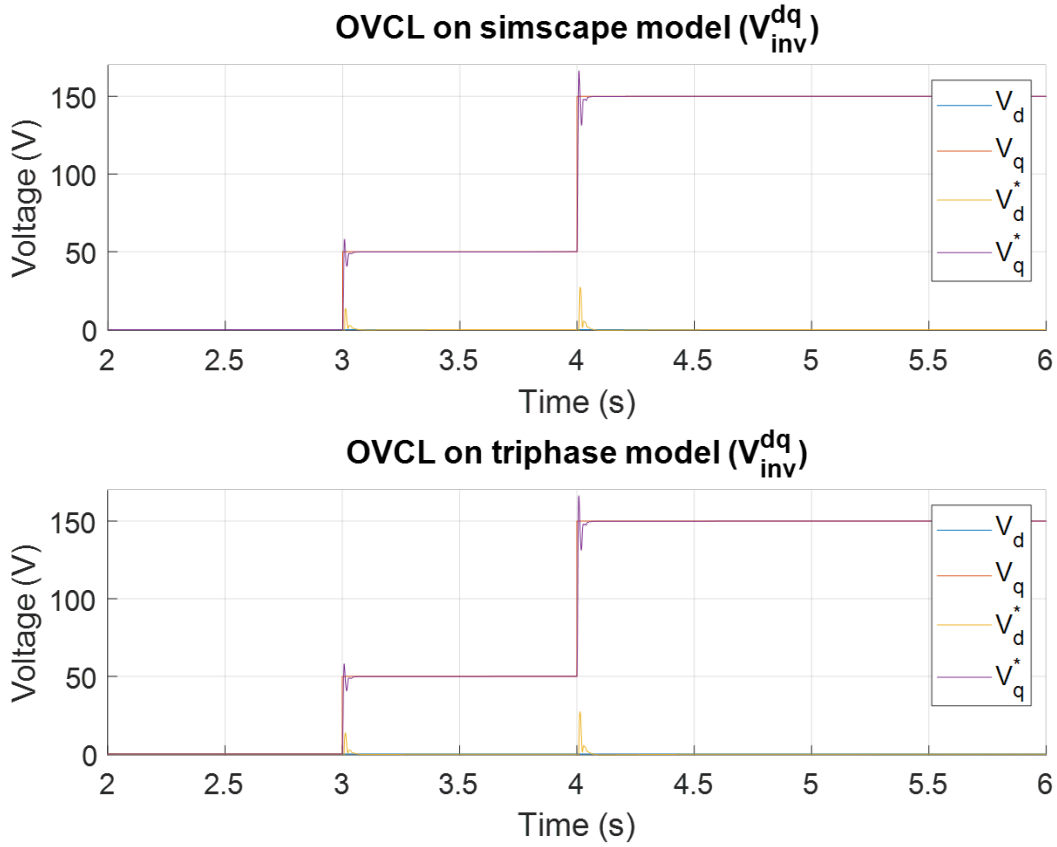

Figure 5: Top plot. Dynamic response of the voltage control loop under step reference change of $v_q^\star$ using the simulation files of the User Group. Bottom plot. Dynamic response of the voltage control loop under step reference change of $v_q^\star$ using the simulation files of the Host Group.

the value of the resistance of the load should be included for its calculation since it affects the parameters of the plant, and, therefore the tuning of the controller. In addition, the dynamic introduced by the filter in order to obtain the virtual *dq* axes also affects the dynamic response of the controller. Despite having a slow dynamic, this result is considered satisfactory since it allows to control the currents in the rotating frame *dq* and, in addition, the reasons of the slow dynamic response is known.

The steady-state ac current injected from the power converter is depicted in Fig. 8. It is observed that the value of the peak current is 2 A, which coincides with the reference current $I_q^\star$. The current contains a total harmonic distortion (THD) of 14.58%, with the 3rd, 5th and 7th harmonics being the most relevant. This poor quality occurs because the converter is being operated at a very low state of charge compared to its rated power (15 kVA). Therefore, the harmonics present in the system, mainly due to the PWM dead-time, affect the power quality to a greater percentage with low currents. The converter state of load cannot be increased because there are limitations with the power that can be provided from the DC bus, which is powered by batteries with a very low nominal current.

Fig. 9 shows the tracking of the reference and the steady-state current under a reference step change of 2 A peak value when the current control loop is implemented in stationary frame. This is also characterised by a slow dynamic response due to the fact that the tuning of the resonant gain is carried out in a similar way to the integral gain of the PI control, that is, only the internal resistance of the inductor is taken into account, obviously the resistance of the load,

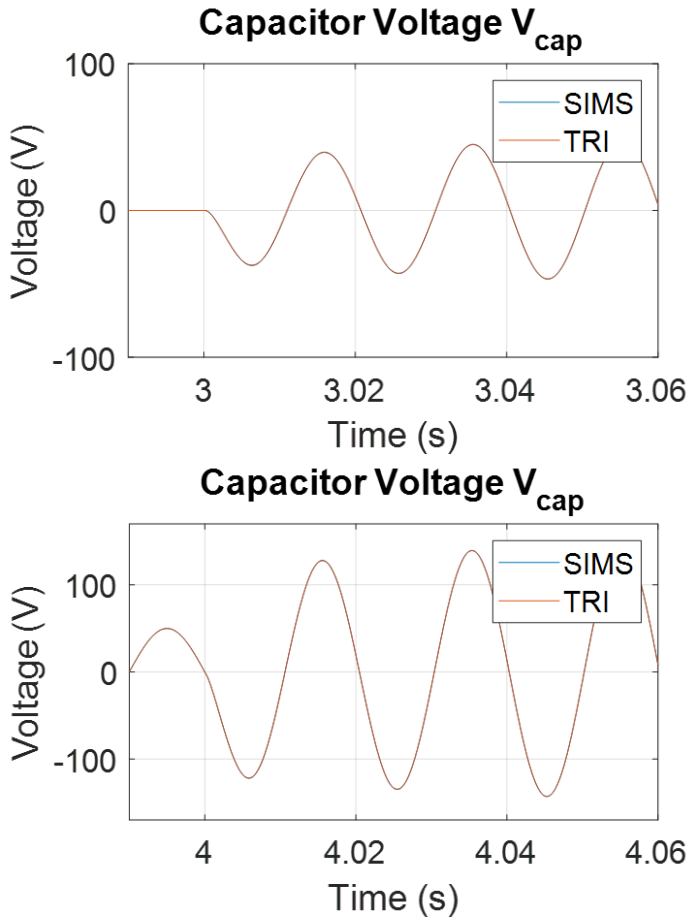

Figure 6: Capacitor voltages comparison in stationary frames between simulations of the user group and host group.

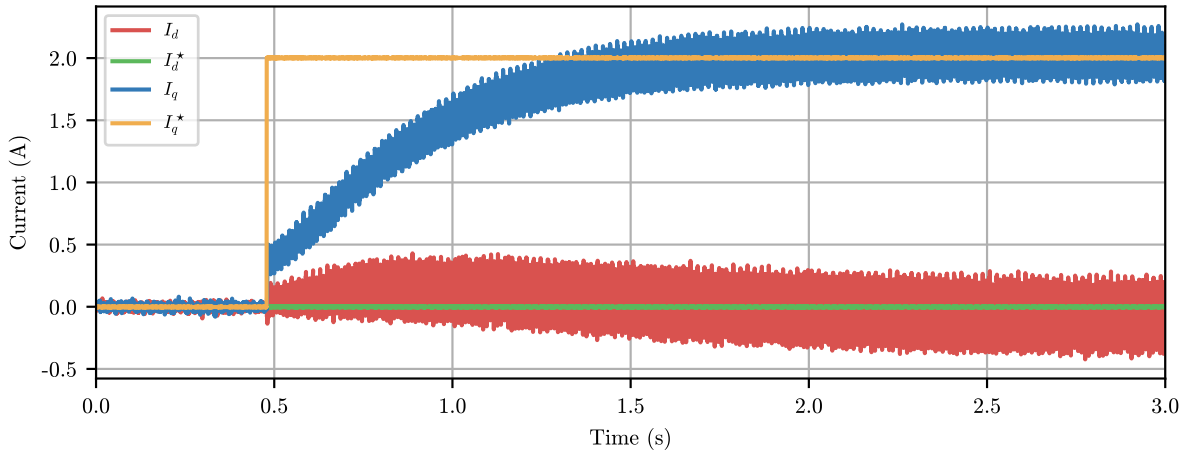

Figure 7: Dynamic performance of the current control loop in statinary frame. Tracking of the currents $I_d^\star$ and $I_q^\star$

which is much greater. However, this controller does no contain any delay relative to the filter of the signals since the PR controller is applied directly to the error of the measured current. The steady-state is reached in about 2 seconds as shown in the left side of the figure. The right

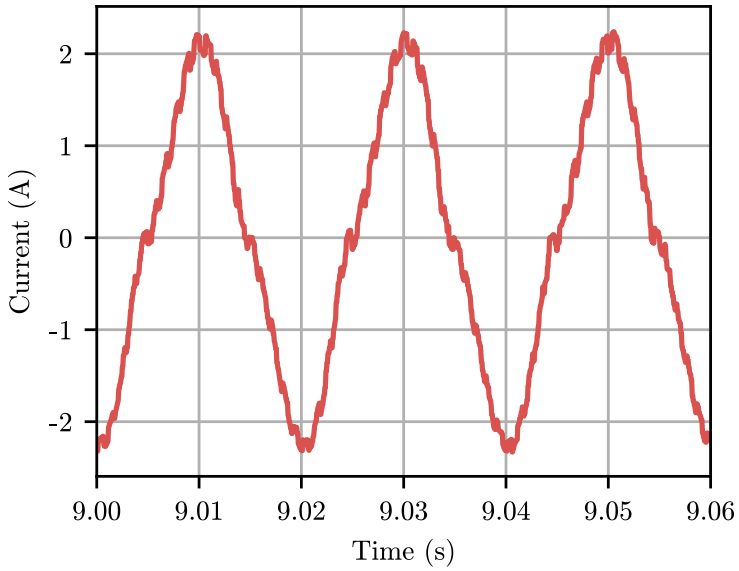

Figure 8: Steady state of the current delivered to the load by the VSC in rotating frame.

side presents three cycles of the current when the stationary-state is achieved. This current contains a total harmonic distortion equal to 14.09% which is very similar to the THD of the rotating reference frame.

It can be concluded that the dynamic response and steady state yields similar results between both reference frames for the current control loop.

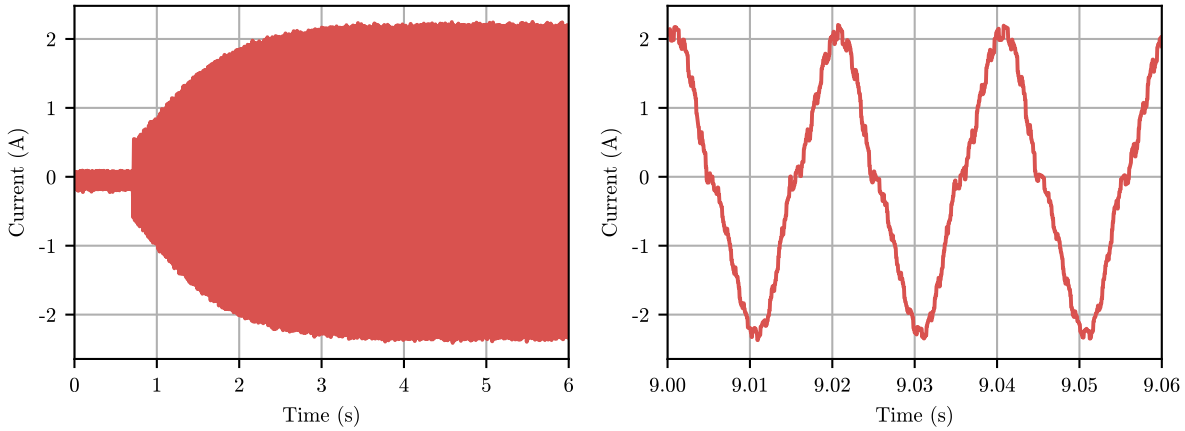

Figure 9: Left plot. Dynamic response of the current control loop in stationary frame under 2 A step reference change. Right plot. Steady state response of the current control loop in stationary frame.

4.1.2 Voltage control loop

This section is devoted to evaluating the validation of the voltage control loop in both reference frames. To do this, proceed in the same way as in the previous subsection. Firstly, the dynamic response of the controller is analysed and, then, the steady-state response.

The evolution of the voltage in the rotating frame *dq* is illustrated in Fig. 10 under a reference

step change from 320 V to 0 V for the component $V_q^\star$. A fast dynamic response is observed in the voltage V_q that reaches the reference in less than 0.1 s. This control imposes the capacitor voltage and, therefore, the resistor voltage. This means that the resistance value is not significant for the performance of this control level achieving a fast dynamic response. The dynamic behavior presents a higher order response with an overshoot and oscillation. This is mainly due to the filter introduced on the signals to obtain the virtual rotating frame *dq* whose dynamics significantly affect the transient response of the controller. In addition, this filter also affects the coupling degree with respect to the component V_d. A large distortion appears at the beginning of the step change reference although is quickly mitigated. The dynamic behavior of the voltage signal accross of the capacitor is shown in the left side of Fig. 11. This shows the same response as its components in *dq*, clearly observing a small overshoot in the voltage until reaching 0 V.

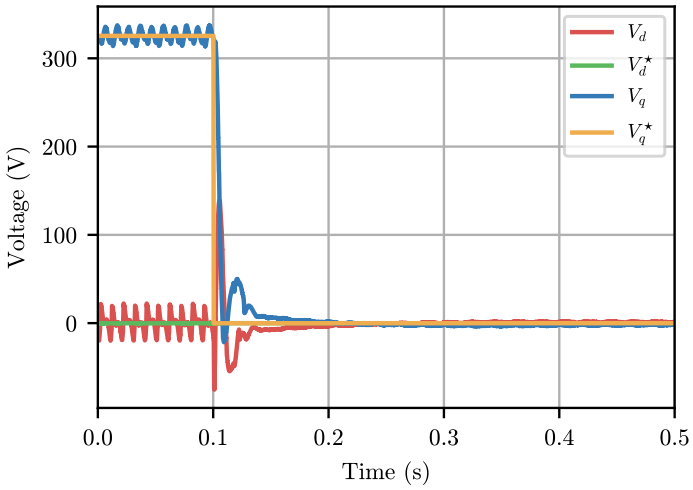

Figure 10: Dynamic response of the voltage control loop in rotating frame for a step change of the reference $V_q^\star$ from 320 to 0V.

The steady-state ac voltage imposed across the capacitor is represented in the right side of Fig. 11. As can be seen, the peak value of the voltage is 320 V, which coincides with the voltage reference $V_q^\star$ at the beginning of test in Fig. 10. The total harmonic distortion is 3.27% reaching a good power quality since the converter is being operated at its rated voltage.

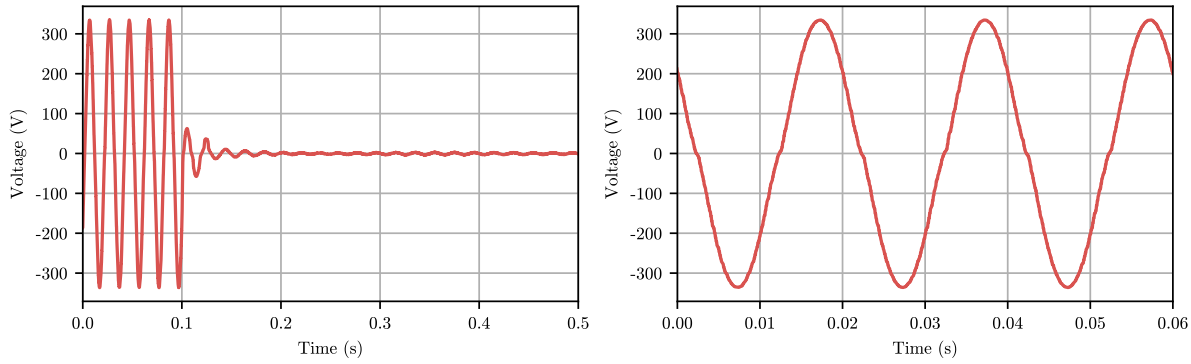

Figure 11: Voltage across the capacitor for a step change of the reference $V_q^\star$ from 320 to 0V in rotating frame. Left side: Transient behaviour. Right side: Steady-state voltage.

Identical test was performed in the stationary frame, that is, a reference step change from 320 V to 0 V of the voltage reference. The left side of the Fig. 12 represents the evolution of the voltages across the capacitor under this reference change. A fast dynamic response is observed with some slight oscillation and the steady-state is reaching in just over 0.05 s. This response is somewhat faster than the one presented in the rotating framework. The main reason is that the controller in stationary frame is implemented without applying any filter to the current and voltage measurements. Therefore, no additional dynamics are introduced that affect the response of the controller. The steady-state voltages are illustrated in the right side of Fig. 12. This corresponds to the voltages at the beginning of the test. A predominantly sinusoidal signal is observed at 50 Hz with a THD of 3.05% which is very similar to that obtained in the rotating frame.

Again, the dynamic and steady state response is similar between both reference frames for the voltage control loop. The only appreciable difference is a somewhat faster dynamic response in the stationary reference frame.

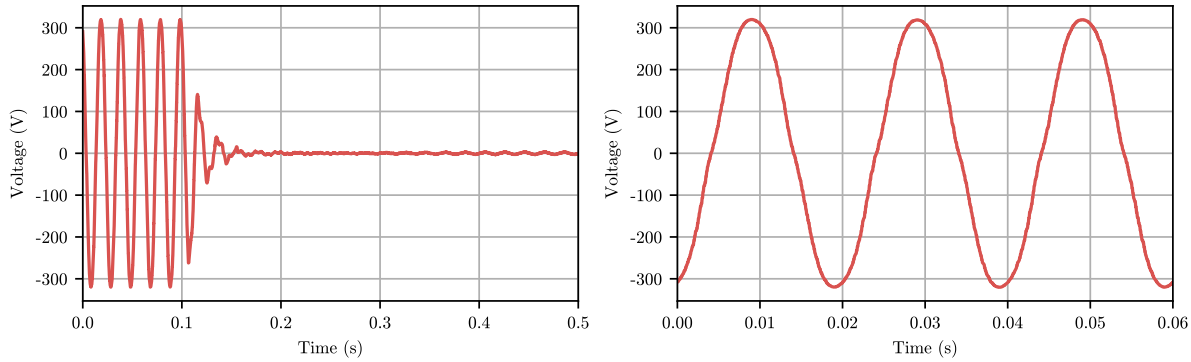

Figure 12: Voltage across the capacitor for a step change of the reference $v_m^\star$ from 320 to 0V in stationary frame. Left side: Transient behaviour. Right side: Steady-state voltage.

4.1.3 Secondary/Primary controllers and VSG

This section evaluates all control levels of the single-phase GF VSC implemented in rotating and stationary frames. The performance of the controllers are evaluated in the event of a change in power supplied to the resistive load. To subject the system to a load change and analyze the GF response, a step change will be made to the reference of the virtual electromotive force e^*, see Fig. 1 and Fig. 2, from 0 to 320 V. This will cause the voltage across the load changes suddenly and an increase in the power demanded by the resistive load. The reason for establishing this strategy to subject the system to a load change is because there are no additional resistors in the laboratory of the host group to vary the load connected to the Triphase converter.

The active power injection p from the power converter and its reference $p^\star$ computed by the primary and secondary controller are shown in the left side of Fig. 13 for the virtual rotating frame dq. A power increase corresponding to the step change of $e^\star$ is observed. The dynamic power response of p and $p^\star$ evolves smoothly until the steady state is reached around 5 seconds of testing. The right side of the figure represents the frequency evolution during the test. At the beginning of the test, the system is in steady-state and the frequency is constant and established at the fundamental value ($2\pi 50$). When the power increase occurs, it is observed

that the frequency is drastically reduced until it gradually recovers until reaching the nominal frequency again. This occurs when p and $p^\star$ are coincident. The evolution of the frequency allows to observe the behaviour of the control under load variations. The first instants of the transient response up to its minimum value correspond to the inertial response of the VSG. Then the frequency begins to rise thanks to the action of the primary control and, later, the frequency returns to its original value due to the action of the secondary controller.

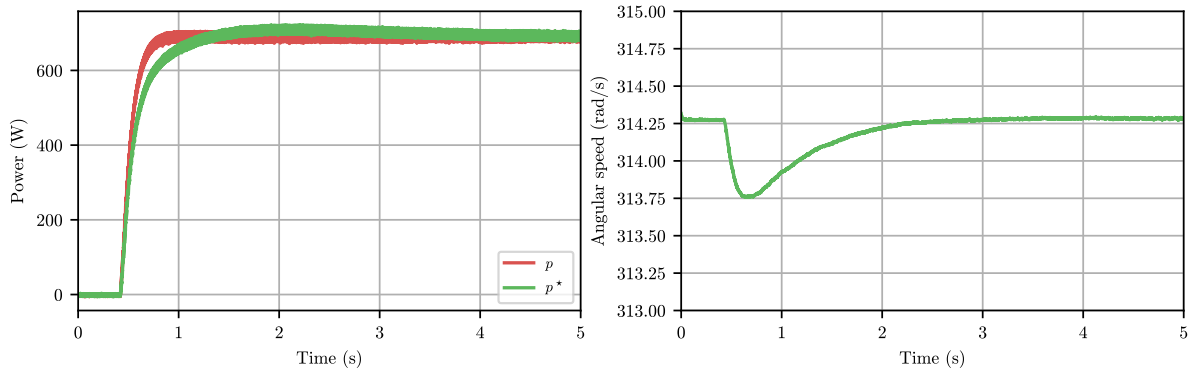

Figure 13: Left side: Active power p injected by the VSC and active power $p^\star$ for a step change of $e^\star$ from 0 to 320V in rotating frame. Right side: Frequency evolution of the system under a step change of $e^\star$ from 0 to 320V in rotating frame.

The evolution of the instantaneous voltage in the transient and steady-state is illustrated in Fig. 14. During the transient response, the voltage evolves with a smooth response similar to a first order response until steady state is reached in about 4-5 cycles of the fundamental frequency. The voltage in steady-state shows a good power quality with an almost perfect sinusoidal signal which is reflected in a THD lower than 1.26%.

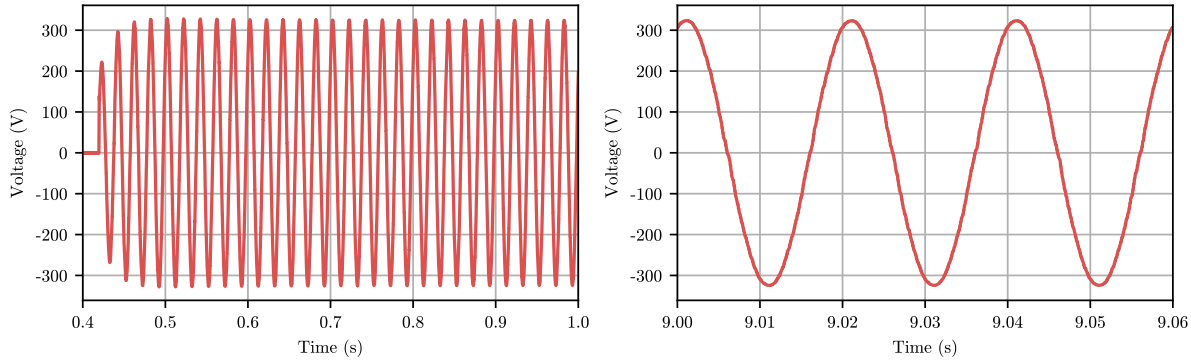

Figure 14: Voltage across the capacitor fro a step change of $e^\star$ from 0 to 320V in rotating frame. Left side: Transient response. Right side: Steady-state response.

Identical test was performed for the stationary reference frame. The evolution of power p is shown in the left side of Fig. 15. Once again, an abrupt increase in power is observed as a consequence of the step change of $e^\star$. The power evolves smoothly with a slight overshoot and a faster dynamic response, that is, the permanent regime is reached before the rotating frame around 3 seconds of tests. On the right side of the figure the evolution of the frequency is shown. It clearly identifies the inertial response of the system, corresponding to the first moments of the event, the primary response that allows the frequency to be raised, and the secondary control that returns the frequency to its fundamental value. However, it is important

to mention that this process occurs faster than the rotary frame because the active power reaches its reference faster. The main reason for this better performance of the stationary frame with respect to the rotating frame is found in the filter of the virtual *dq* axes. This introduces a delay that makes the response of the rotary frame slower as explained in the simulation results.

Finally, it is important to highlight that the minimum value of frequency reached in this test is lower than the minimum value of frequency in the rotating frame. Just the opposite occurs in the simulation results. Nowadays, the reasons for this difference are unknown, therefore, further analysis and research have to be carried out on these experimental results and their implementation to find this difference with respect to the simulation results. The evolution of

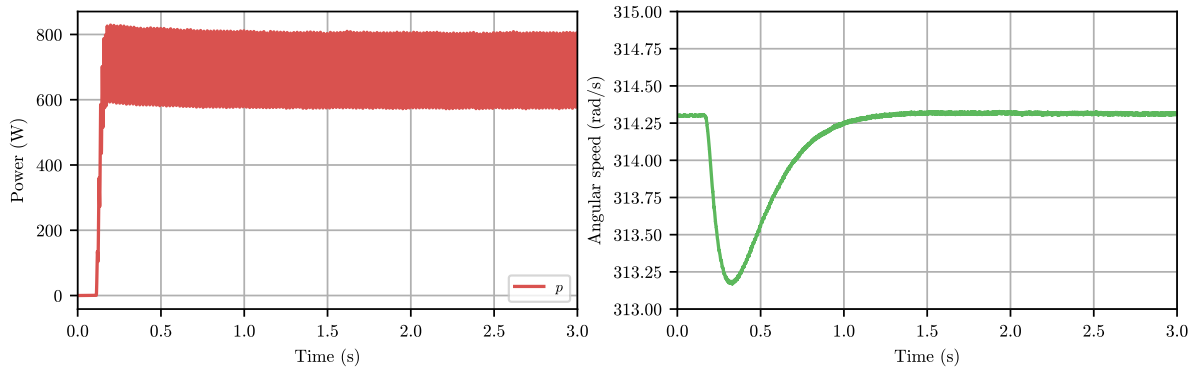

Figure 15: Left side: Active power p injected by the VSC and active power $p^\star$ for a step change of $e^\star$ from 0 to 320V in stationary frame. Right side: Frequency evolution of the system under a step change of $e^\star$ from 0 to 320V in stationary frame.

the voltages during the transient and steady-state regime are shown in Fig. 16. A fast dynamic response with a slight overshoot is observed. The voltages in permanent regime show a good power quality with a THD of 1.74% similar to that reached in the rotating axes.

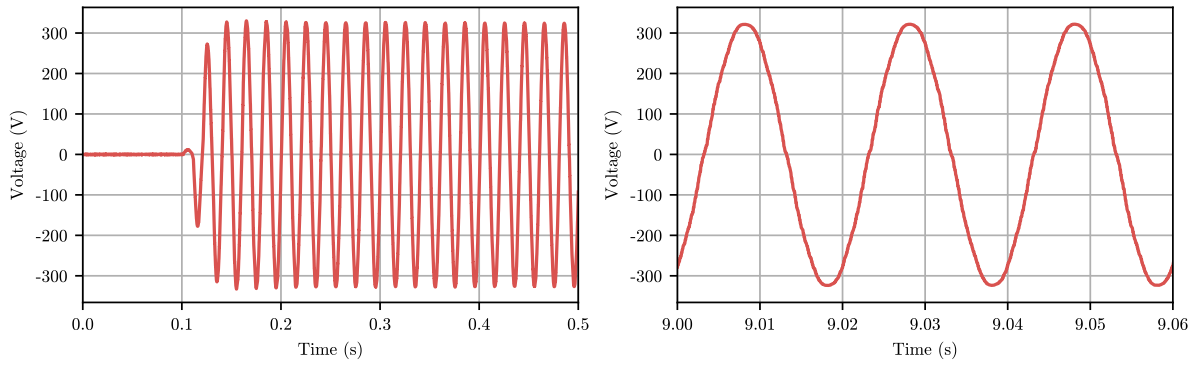

Figure 16: Voltage across the capacitor fro a step change of $e^\star$ from 0 to 320V in stationary frame. Left side: Transient response. Right side: Steady-state response.

4.1.4 P-HIL investigations for emulating a passive load

P-HIL is a technique based on the physical emulation of a simulated voltage by means of a power amplifier. This allows connecting a VSC to the amplifier and studying its behavior under

events in the simulated system which will be reproduced by a variation in the voltage imposed by the amplifier. However, in the case of the single-phase GF VSC operating in isolated mode this procedure is not valid since its objective is to impose the voltage on the POI of the converter. Since the voltage is imposed by the GF VSC, it is proposed to operate the amplifier as a current source instead of voltage source. In this way, the current absorbed by the load connected to the POI of the converter can be emulated. This form of operation is the first time that it was considered in the infrastructure of the host group laboratory, therefore, a strategy was established to evaluate the behavior of the amplifier as a current source as well as the stability study of the P-HIL. This consisted of the following stages:

- Emulate a P-HIL environment in a simulated environment modeling all the devices involved and the delays present in the system.
- Evaluate various strategies for implementing a current source in the amplifier. These will be evaluated in the simulated environment of the previous step. Among them, the following have been considered: i) measuring the POI voltage imposed by the GF VSC in RTDS, feeding a load in RTDS with that voltage and measuring the current circulating through the load so that it is reproduced by the amplifier. ii) Integrate a PI controller to control the current absorbed by the load. The output of the PI control would correspond to the voltage imposed by the amplifier.
- Select the strategy that offers the best performance to be carried out in the experimental test P-HIL.

During the development of the project, the simulated model of P-HIL was carried out and the two strategies that have been proposed were discussed between both groups. Therefore, its validation through simulation and experimental implementation was pending. To complete this part of the work, we have participated in a new ERIGrid 2.0 call for this year 2023.

4.2 Conclusions

This work has presented the experimental validation of a single-phase GF VSC operating in isolated mode for two reference frames: rotating and stationary frames. Both controls have been validated through the User Group's own simulations, adaptation of these simulations to the Host Lab's simulation environment, which faithfully represents the experimental equipment they have, and finally, experimental validation using the experimental equipment of the host group. During this development process the following milestones have been reached between both groups.

- The host group has transferred their knowledge in the implementation of C-HIL and P-HIL controls, especially those related to stability due to the delay in the implementation loop.
- The host group has transferred their knowledge to the User Group on the use of commercial power converters such as Triphase and the real-time RTDS control platform interconnected to the amplifier to perform P-HIL.
- User group has transferred its knowledge of control of the GF converter to the host group.
- The user group has transferred its knowledge in converter control and power quality improvement to the host group.
- Both groups have collaborated extensively to adapt the model for single-phase GF VSC which has involved discussions ranging from control strategies to simulation file transfer.

- A work methodology has been developed to implement the control of power converter between both groups. This includes: i) simulation validation by the User Group, ii) transfer of these simulation to the Triphase platform of the Host Group for validation and evaluation and, iii) experimental validation of the control. Between one stage and another, comparisons are made both in steady and transient states to evaluate the performance of the controller.
- An accepted abstract for the conference SEST'23 relative to this work. The submission of the full paper is April 14, 2023.

With respect to the results obtained, it can be concluded that both controllers present a good performance to implement single-phase GF VSC. However, the stationary frame avoids introducing delays in the control magnitudes which leads to a faster dynamic response.

5 Open Issues and Suggestions for Improvements

Throughout the development process of the project, an identical behavior has been observed between simulations and experimental results. The only disagreement has been that the minimum value of the frequency in experimental results is lower for the stationary frame. While, in the simulations this value is lower in the rotating frame. This discrepancy has remained pending study. Both groups believe that the value of some of the controller gains must be different between the simulations and the experimental results causing this difference. However, it requires further analysis to find the reason for this discrepancy.

In addition, it has been pending to implement the emulation of the behavior of a resistor in P-HIL through RTDS and the amplifier. There are several proposals by both groups which are mainly oriented to emulate the current circulation of the load through the amplifier.

For future research, both groups have been discussing the extension of GF VSC in grid-connected mode. This part requires an adjustment of the controller gains that ensures stability of the system under different R/X ratios of the network.

Taking into account all these open questions, the User Group has participated in a new Erigrid 2.0 call in 2023 with the aim of resolving and implementing solutions of these challenges together with the Host Group.

References

Hu, J., Shan, Y., Cheng, K. W., & Islam, S. (2022). Overview of power converter control in microgrids—challenges, advances, and future trends. *IEEE Transactions on Power Electronics*, *37*(8), 9907-9922.

Kryonidis, G. C., Malamaki, K.-N. D., Mauricio, J. M., & Demoulias, C. S. (2022). A new perspective on the synchronverter model. *Int. J. Electr. Power Energy Syst.*, *140*, 108072. doi: https://doi.org/10.1016/j.ijepes.2022.108072

Liao, Y., & Wang, X. (2019). Evaluation of voltage regulators for dual-loop control of voltage-controlled vscs. In *2019 ieee energy conversion congress and exposition (ecce)* (p. 5036-5042). doi: 10.1109/ECCE.2019.8912561

Liao, Y., Wang, X., Liu, F., Xin, K., & Liu, Y. (2019). Sub-synchronous control interaction in grid-forming vscs with droop control. In *2019 4th ieee workshop on the electronic grid (egrid)* (p. 1-6). doi: 10.1109/eGRID48402.2019.9092640

Loh, P. C., & Holmes, D. (2005). Analysis of multiloop control strategies for lc/cl/lcl-filtered voltage-source and current-source inverters. *IEEE Transactions on Industry Applications*, *41*(2), 644-654. doi: 10.1109/TIA.2005.844860

Matas-Díaz, F. J., Barragán-Villarejo, M., Olives-Camps, J. C., Mauricio, J. M., & Maza-Ortega, J. M. (2022). Virtual conductance based cascade voltage controller for vscs in islanded operation mode. *Journal of Modern Power Systems and Clean Energy*, *10*(6), 1704-1713. doi: 10.35833/MPCE.2021.000121

Ndreko, M., Rüberg, S., & Winter, W. (2020). Grid forming control scheme for power systems with up to 100% power electronic interfaced generation: a case study on great britain test system. *IET Renewable Power Generation*, *14*(8), 1268-1281. Retrieved from https://ietresearch.onlinelibrary.wiley.com/doi/abs/10.1049/iet-rpg.2019.0700 doi: https://doi.org/10.1049/iet-rpg.2019.0700

Ooi, B., & Wang, X. (1990). Voltage angle lock loop control of the boost type pwm converter for hvdc application. *IEEE Transactions on Power Electronics*, *5*(2), 229-235. doi: 10.1109/63.53160

Rocabert, J., Luna, A., Blaabjerg, F., & Rodríguez, P. (2012). Control of power converters in ac microgrids. *IEEE Transactions on Power Electronics*, *27*(11), 4734-4749. doi: 10.1109/TPEL.2012.2199334

Rodriguez, P., Candela, I., Citro, C., Rocabert, J., & Luna, A. (2013). Control of grid-connected power converters based on a virtual admittance control loop. In *2013 15th european conference on power electronics and applications (epe)* (p. 1-10). doi: 10.1109/EPE.2013.6634621

Rodríguez, P., Citro, C., Candela, J. I., Rocabert, J., & Luna, A. (2018). Flexible grid connection and islanding of spc-based pv power converters. *IEEE Transactions on Industry Applications*, *54*(3), 2690-2702. doi: 10.1109/TIA.2018.2800683

Rosso, R., Wang, X., Liserre, M., Lu, X., & Engelken, S. (2021). Grid-forming converters: Control approaches, grid-synchronization, and future trends—a review. *IEEE Open Journal of Industry Applications*, *2*, 93-109. doi: 10.1109/OJIA.2021.3074028

Zhang, L., Harnefors, L., & Nee, H.-P. (2010). Power-synchronization control of grid-connected voltage-source converters. *IEEE Transactions on Power Systems*, *25*(2), 809-820. doi: 10.1109/TPWRS.2009.2032231

Zhong, Q.-C., & Weiss, G. (2011). Synchronverters: Inverters that mimic synchronous generators. *IEEE Transactions on Industrial Electronics*, *58*(4), 1259-1267. doi: 10.1109/TIE.2010.2048839

Disclaimer

This document contains material, which is copyrighted by the authors and may not be reproduced or copied without permission.

The commercial use of any information in this document may require a licence from the proprietor of that information.

Neither the Lab Access User Group as a whole, nor any single person warrant that the information contained in this document is capable of use, nor that the use of such information is free from risk. Neither the Lab Access User Group as a whole, nor any single person accepts any liability for loss or damage suffered by any person using the information.

This document does not represent the opinion of the European Community, and the European Community is not responsible for any use that might be made of its content.

Copyright Notice

This project has received funding from the European Union's Horizon 2020 research and innovation programme under Grant Agreement No. 870620.